International Journal of Engineering Inventions
e-ISSN: 2278-7461, p-ISSN: 2319-6491
Volume 13, Issue 3 [March. 2024] PP: 65-84

Characteristics of blended geopolymer concrete and its performance evaluation for pre-cracked RC-beams as a repairing and strengthening materials

Mariam Farouk Ghazy[1], Mohamed Helmy Taman[2], Sara Saad ELatfawy[3]
[1,2] *Professor, Structural Engineering Department, Faculty of Engineering, Tanta University, Tanta, Egypt*
[3] *M. Sc. Student, Structural Engineering Department, Faculty of Engineering, Tanta University, Tanta, Egypt*

Abstract
In the construction industry, the repair and strengthening of damaged concrete structures is a crucial task. Many concrete structures are deteriorating, sometimes at early ages, and require rehabilitation to restore their serviceability and protection. Consequently, there has been a significant increase in the requirement for safety and repair in recent times.
This study aims to study the characterization of blended geopolymer concrete (GPC) as a repairing and strengthening material for Portland cement concrete (PCC) substrate. A total of four GPC mixes were created using different proportions of fly ash (FA): ground granulated blast furnace slag (GGBFS) (100%:0, 50%:50%, 25%:75%, and 0%:100%). A combination of potassium silicate (KS) solution and sodium hydroxide (NH) solution (16M) was used as the alkaline solution for the polymerization process in this study. The PCC mix was made in parallel with the GPC mixes for preparing the control mix. The compressive, splitting, flexural, bond strengths and modulus of elasticity for all mixes were evaluated at 3, 7 and 28 days. As well as slant shear and pull-off tests were conducted to evaluate the bond strength of GPC and PCC substrate at different surface condition at 3 and 28 days. For the purpose of evaluation of the performance of the method of using GPC as repair and strengthening material, reinforced concrete beams were cast, damaged at two levels fully damaged and partially damaged up to 45% and 75% of its ultimate loads, respectively strengthened and tested using static flexural loading.
The results show that the mechanical properties of blended GPC is higher than those depicted for FA-based GPC and PCC. Moreover, using 50% GGBFS lead to high early strength, at 3 and 7 days develop strength of about 74% and 93% of that at 28 days, respectively. From the slant shear test results, GPC with 50% GGBFS had good shear bond strength to the cementitious concrete. In addition, in case of dry substrate surface enabled the geopolymer repair concrete to achieve higher shear bond strength than depicted in the case of wet surface case. The findings from the bond strength analysis indicate that incorporating GGBFS and FA in concrete mixes can be a viable approach for repairing and strengthening environmentally sustainable concrete. Blended GPC with 50 % GGBFS has strong potential to be used as repairing and strengthening material for deteriorated reinforced concrete structures. On the other hand, repaired partially damaged RC beams exhibited better behavior than repaired fully damaged RC beams. In addition, the ductile behaviour of repaired RC beams was better than that of the controlled RC beams.
Keywords: *Geopolymer concrete, Mechanical properties, Bond strength, Repairing and strengthening material, Slant shear, Pull-off.*

Date of Submission: 02-03-2024 Date of acceptance: 11-03-2024

I. Introduction

The second-most frequently used material worldwide is concrete. Even though it is renowned for having good mechanical and durable properties, some buildings are beginning to deteriorate almost 30 years after construction. In order to solve this problem, researchers are competing to develop more cost-effective and environmentally friendly materials. Geopolymer binder is one of the recent solutions for this problem. Geopolymer is thought to be a good fit since it creates a greener construction material by using recycled industrial waste as a binding material in combination with an alkali reactant [1]. The use of geopolymer demonstrated significant environmental benefits, including reduced CO_2 emissions, energy conservation, and sustainability [2]. The manufacturing of 1 m^3 of concrete results in CO_2 emissions of 354 kg CO_2-eq, of which 269 kg CO_2-eq (76%) come from the production of cement [3], around 70% fewer gas emissions are produced by geopolymer concrete (GPC) than by Portland cement [4].

Fly ash (FA) and ground granulated blast furnace slag (GGBFS) are both by-products from other operations, and using them in GPC can enhance its properties [5]. GGBFS and FA are less expensive materials than silica fume [6]. Many studies on FA-based GPC have been conducted, primarily using low-calcium FA [7-9]. The chemical composition of GGBFS is depending on the chemical composition of the raw materials used for producing iron. A solution of sodium hydroxide (NaOH) and sodium silicate (Na_2SiO_3) is the most popular alkaline liquid used in geopolymerization. However, potassium hydroxide (KOH) and potassium silicate (K_2SiO_3) can be used also [10]. In GPC, the precursor, alkaline solution, and curing regime all have a substantial impact on shrinkage. For instance, the self-desiccation of concrete causes significant autogenous shrinkage in Portland cement concrete (PCC), whereas continuous reorganization and polymerization of the gel structure causes minimal autogenous shrinkage in GPC [11,12]. Due to high capillary pressure brought on by self-desiccation coupled with a high degree of hydration, slag-based GPC has been associated with substantial autogenous shrinkage [13]. In order to overcome the issue of shrinkage that may occur when employing geopolymers for repair applications, adding internal short fibers was suggested [13,14].

Repair materials based on geopolymers perform better than those based on cement [2]. Therefore, geopolymer must meet the repair standards, much like any commercial repair material, or perform better, including having better fresh and mechanical properties and good bond strength [2,15]. The compressive strength is the property that attracts the most attention in structural applications. Geopolymer concrete gain strength with time in ambient conditions, as seen with PCC [16]. However, heat curing from 0° C to 150° C greatly increases compressive strength [17] where, depending on the curing temperature, complete compressive strength could be attained in few days [16,18]. The use of geopolymers as protective coating materials for marine concrete and transportation infrastructure has increased over time [19]. However, when choosing geopolymers as repair materials, the bond strength between the substrate concrete and the repair material is crucial [20,21]. Several researchers [22,23] tested their slant shear, pull-out, and direct shear tests in an effort to use geopolymer as a repair material. The bond strength between the mortar substrate and the geopolymer in sandwich specimens was investigated and as a result, the bond strength of geopolymer was greater than that of an equivalent PCC mixture [22].

The efficiency of using geopolymer cement as a concrete building repair material has been demonstrated by several investigations. Activated alkali geopolymer pastes were used to fill inclined cracks in concrete structures [24]. The paste was made of FA and GGBFS, after the repair, examination revealed that the failure occurred in the concrete substrate, demonstrating the paste's higher strength [24]. A geopolymer automated sensor coating for structural repairs was created [25]. Among other research in this field, 2-m-long double reinforced cement concrete beams were repaired using GGBFS and low-calcium FA-based geopolymer [26]. The repaired beam with GPC had a higher flexural strength than the one with PCC. A new type of geopolymer-based composite piles with geogrid, polyvinyl chloride (PVC), and fiber-reinforced polymer (FRP) was also developed [27], and used to strengthen the shear of reinforced concrete beams. These piles had a higher resistance than PPC. A method for repair using geopolymer mixture prior to This work was presented [28]. Geopolymer reinforced with steel fibers was utilized [29] to increase the structural strength of reinforced concrete buildings. Additionally, the researchers used GPC consisting of metakaolin and FA classes F and C to repair buried infrastructure. There is evidence to support the use of GPC in new or repaired structures to combat corrosive environments [30]**.**

Previous research has highlighted the potential benefits of geopolymer as a sustainable building material and for repair and strengthening purposes. Some researchers have focused on developing geopolymers using raw materials like FA, metakaolin, silica fume, and GGBFS. However, there is limited research addressing the mechanical properties and bond properties of geopolymer composites as repair and strengthening materials for PCC substrate. This study aims to investigate the fresh and hardened properties of blended geopolymer concrete, including compressive strength, splitting tensile strength, flexural strength, bond strength, modulus of elasticity, and bonding mechanism against PCC substrate. Hence, repair and strengthening of RC beams were performed using blended GPC.

II. Experimental program

2.1 Material properties

Materials used in this study were obtained from local Egyptian sources that are commonly used in Egyptian constructions. The properties of the used materials are detailed in the following:

Fly Ash: Low-calcium FA (class F) according to **(ASTM C 618-012a)** [31] with specific gravity 2.4 was used as a source of pozzolanic material to produce geopolymer concrete.

Ground Granulated Blast Furnace Slag: GGBFS comply with **(ASTM C989-94)** [32] requirement**s,** which was gathered from a local distributor with specific gravity 2.9 were chosen to create the GPC mixes.

Cement: Portland cement (PC) CEMI 42.5N was used to prepare the control mix and substrate concrete. The used cement complied with the requirements of (**EN 196-1:2016)** [33] **and (ES 4756-1:2022)** [34].

Table 1 displays the chemical composition of the used FA, GGBFS and PC as determined by (XRD) test.

Aggregates: River siliceous medium well-graded sand (S) was used as a fine aggregate in the experimental program for all concrete mixes according to **(ECP 203/2019)** [35] and **ASTM C33/C33M** [36] with a specific gravity of 2.6, a fineness modulus of 2.33 and water absorption 0.9%. Whereas the crushed dolomite was used as a coarse aggregate (CA) for all concrete mixes with maximum size 10 mm and specific gravity 2.55.

Alkaline solution: To achieve good workability, the used alkaline solution was a combination of potassium silicate K_2SiO_3 (KS) and sodium hydroxide NaOH (NH) as recommended by **Ghazy et al., 2022** [37]**.** The used NH were in pellet form with 98-99% purity and KS which chemical composition was provided by the manufacturer is as follows: (Molar ratio SiO_2/K_2O = 2, K_2O= 14-15%, SiO_2= 29-30% and water = 58% by mass), the solution viscosity is equal to 450 MPa.s, and its specific gravity is 1.4 g/ML. The dissolved mass of NH depending on the concentration of solution expressed in terms of Molar (M). In this study NH solution with a concentration of 16 M was used and the KS/NH ratio was 2.5.

Water: The tap water contributed in accordance with the specifications of **(ECP 203-2019)** [35], was used to prepare the NH solution and for mixing and curing the PCC samples. Also, it was used as extra water in GPC mixes.

Superplasticizer (SP): SP of modified polycarboxylates in the form of a clear liquid with a density of approximately 1.08 kg/liter at room temperature was used to improve the workability of the GPC mixes comply with **ASTM C494** type G and F standards.

Fibers: polypropylene fibers (PP) were used in all geopolymer mixes with a volumetric ration of 0.1%. **Table 2** illustrates the properties for PP used as given by the supplier.

Steel reinforcement: Steel reinforcement rebars with diameter 10 mm which is compatible with **ES 262-1 (2015)** [38] was used to evaluate the bond strength by using the pull-out test specimens as well as used as the tension (bottom) and compression (top) reinforcement for beam specimens, respectively. Furthermore, steel reinforcement rebars with diameter 8 mm was used for shear reinforcement (stirrups). **Table 3** presents the properties of used steel bars.

Epoxy resin: adhesive is a medium – viscosity 2 components product based on modified epoxy resin was used for bonding new to old concrete in repair and strengthening works.

Table 1: Chemical compositions of the used FA, GGBFS and PC

Oxide %	FA	Limits (ASTM C 618-012a)	GGBFS	PC
SiO_2	61	-	41.66	20
Al_2O_3	18	-	13.96	5.20
Fe_2O_3	5.2	-	1.49	3.10
TiO_2	2.08	Not specified	0.58	-
MnO	0.01	Not specified	0.35	-
MgO	1	Not specified	5.35	-
CaO	6	Not specified	34.53	63
Na_2O	0.7	1.50% max	0.49	0.44
K_2O	0.8	Not specified	0.97	0.15
SO_3	2.3	5.0% max	-	3.01
P_2O_5	0.41	Not specified	0.01	-
LOI	0.2	6.0% max	0.05	5.10

Table 2: The properties of PP used as given by the supplier

Fiber type	Diameter (mm)	Length (mm)	Aspect ratio	Density (kg/m^3)	Elastic modulus (MPa)	Tensile strength (MPa)
PP	0.02	12	750	900	3500	550

Table 3: Properties of steel reinforcement bar used

Property	Diameter (mm)	Tensile strength (MPa)	Elastic modulus (GPa)
value	10	530	211
	8	400	202

2.2 Mix proportions and specimens preparations

In this investigation study, four GPC mixes were prepared using absolute volume method with different percentages of FA: GGBFS as (100%: 0%, 50%:50%, 25%:75%, 0%:100%). In addition, PCC mix was prepare as a control mix and concrete substrate. **Table 4** displays the proportions of the studied mixes.

For all GPC mixes, the NH solution was prepared before 24 hours of mixing. The alkaline solution was created by adding the NH solution (16 M) to the KS solution with ratio (1:2.5) about an hour before mixing. Firstly, the solution and binder were mixed together for 2 minutes in drum mixer with capacity of 100 L. Following that, sand and coarse aggregate were added and continue mixing for further 2 minutes, then SP and extra water were added to the mix and continue mixing for 2 minutes. PP fibers were then manually added, and the mixture was continuously mixed with the mixer until assure the uniformity of the mixture.

For PCC mix, coarse aggregate was added with cement in drum mixer and then mixed in dry state for 2 minutes, water and sand were then alternately added to the cement and coarse aggregate mix for additional 5 minutes to ensure the consistency of the mix.

The fresh concrete was placed in the prepared molds as displayed in **Fig. 1**, and the fresh GPC and PCC were compacted using a mechanical vibrator for 30 s to remove any trapped air.

GPC samples containing FA+ GGBFS were kept in their molds for 24 hrs. However, FA-based GPC samples were kept in their molds for 72 hrs. Samples were removed from the molds and cured with heat in a chamber by putting the samples at a temperature 40 °C for 48 hrs. This temperature degree was chosen to reduce energy consumption and there were several studies recommended it, including **McAlorum,2021** [39]. After the samples have cooled to room temperature, they were placed outdoor in ambient conditions till testing. The outdoor temperatures of the curing period were between February and March in 2022 are shown in **Fig. 2**.

PCC samples were kept in their molds and covered with plastic sheet for 24 hrs at temperature 20±2 ºC and 50% RH, after that the samples were removed from the molds and the curing process took place. Curing of PCC is carried out by covering the sample with wet burlap until the test ages at 3, 7 and 28 days.

On the other hand, the substrate PCC specimens for bond properties were cured for 28 days by being covered with wet burlap. Subsequently, the specimens were exposed to an ambient temperature of 20±2 ºC and 50% RH for an additional 60 days. After a total curing period of 90 days involving water and air exposure, the repair material was applied. The repaired specimens were then subjected to slant shear tests at 3 and 28 days, and pull-off tests at 28 days.

On the other hand, a total of three substrate PCC beams, including a control beam were cast for this study with dimension (150×200×1000) mm and cured for 28 days by being covered with wet burlap. It was reinforced with 2 bars with diameter 10 mm as shown in **Fig. 3.** One of them control and two beam specimens will be loaded with different ratio of its ultimate load. (control beam specimen is prepared to loaded up to failure load, the second beam specimen loaded to 45% of maximum recorded load for control beam specimen, and the third beam specimen prepared to subjected to 75% of maximum load recorded for control beam specimen), respectively.

The cracks that were developed due to the application of load on the RC beams were identified and marked. These cracks were then enlarged using hammer and concrete-breaking bit to facilitate easy and effective application and penetration of repair and strengthening material. The repairing geopolymer concrete mix (F50S50 mix) was applied to fill the cracks till the original cross sectional size of the beam was restored as shown in **Fig. 3**. After that repaired and strengthened beams were cured for another 28 days and tested again.

Table 4: Mix proportions of different concrete mixes

NO	Mix ID	Mix proportions (kg/m^3)										Slump (mm)
		C	FA	GGBFS	S	CA	A		PP	SP	EX/W	
							KS	NH				
1	F100S0	-	400	-	689	1033	171.43	68.6	0.9	-	-	230
2	F50S50	-	200	200	702	1053	171.43	68.6	0.9	2	8	230
3	F25S75	-	100	300	709	1063	171.43	68.6	0.9	6	40	230
4	F0S100	-	-	400	716	1074	171.43	68.57	0.9	12	40	230
5	PCC	400	-	-	642.4	964	-	-	-	-	240	80

Note: C: Cement, FA: Fly ash, GGBFS: Ground granulated blast furnace slag, S: Sand, CA: Coarse aggregate, A: Alkaline solution, KS: Potassium silicate, NH: Sodium hydroxide, PP: Polypropylene fibers, SP: Superplasticizer, EX: Extra water, W: Water. Mix ID(F100S0) refers to: (F) FA with ratio 100% of binder and (S) GGBFS with ratio 0%.

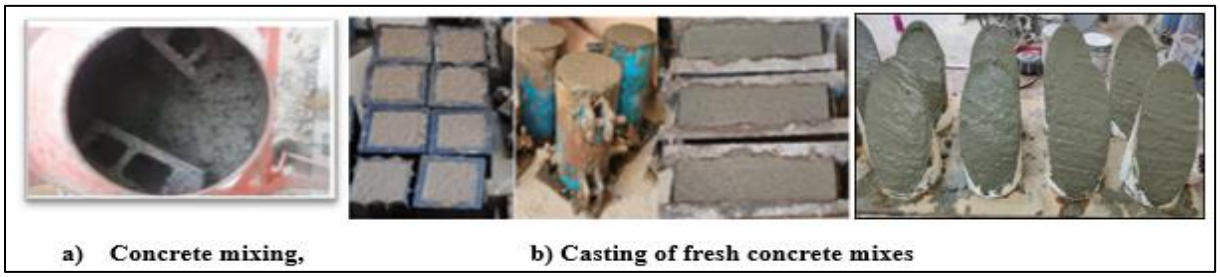

a) Concrete mixing, b) Casting of fresh concrete mixes

Fig. 1: Mixing and casting of concrete mixes

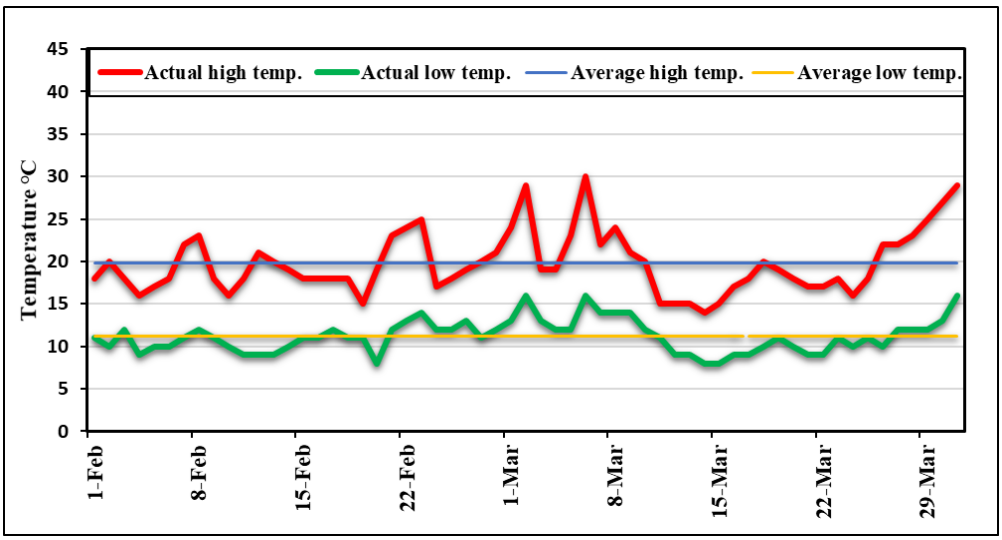

Fig. 2: The outdoor temperature of the GPC curing along month February- March (2022)

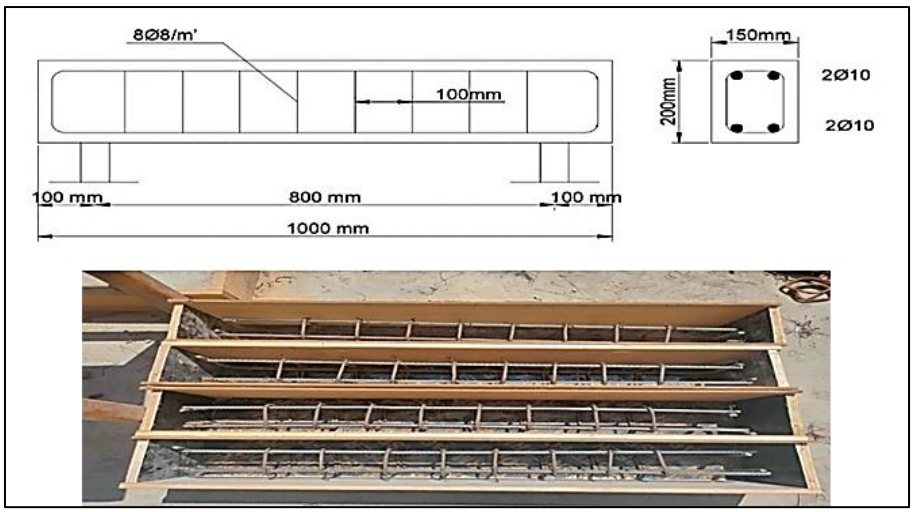

a) Details of reinforcement of concrete beams

b) Concrete beams after casting **c) Repaired and strengthened beam specimens**

Fig. 3: Details of reinforced concrete beam specimens

2.3 Test procedures

2.3.1 Fresh properties of concrete mixes

Testing of the workability of the fresh concrete mix immediately after the process of mixing using slump test according to **ASTM C143** [40].

2.3.2 Mechanical properties of concrete mixes

The mechanical properties: compressive, splitting tensile, flexural strengths, modulus of elasticity and bond strength were measured at different ages. Compressive strength was carried out according to **BS EN 12390-3:2019** [41], using cubic specimens of size (100 ×100 ×100) mm at age of 3, 7 and 28 days. The splitting tensile strength was performed according to **ASTM C39/C39M** [42], on cylindrical specimens of 150 mm in diameter and 300 mm in length, at age of 7 and 28 days. For compressive and splitting tensile strength, a digital hydraulic compression testing machine with a capacity of 2000 kN was used. Moreover, the flexural strength was determined according to **ASTM C78-18** [43], on prism specimens with dimension (100 ×100 ×500) mm and the test was carried out using a Universal Testing Machine of 300 kN capacities at ages of 7 and 28 days. The modulus of elasticity was measured according to **ECP 203/2019** [35], using cylindrical specimens of 100 mm in diameter and 200 in length. The modulus of elasticity test was carried out using a Universal Testing Machine of 300 kN capacities. The pull out test was intended to evaluate the direct bond strength between the steel reinforcing bars and the repair material. Samples were cast into cylinders of dimensions 150 mm diameter and 150 mm height and in its steel bar with diameter 10 mm and tested using Universal Testing Machine of 300 kN capacity after age of 7 and 28 days. The test results for each mix are at least average of three test specimens. Test setup is shown in **Fig. 4**.

a) Compression test b) Splitting tensile test c) Flexure test

d) Modulus of elasticity test f) Bond strength test

Fig. 4: Test setup

2.3.3 Bond properties of GPC with PCC substrate specimens

The following tests were carried out to verify the performance of the conducted concrete overlay and concrete substrate specimens.

2.3.3.1 Slant shear test

The slant shear test is primarily used to measure the bond at the interface between the repair material and the concrete substrate. According to the **ASTM C882** [44] standard, this test procedure was used to evaluate the shear bond strength between old and new concrete. The slant shear specimens were cast into cylinders having a diameter of 100 mm and height of 200 mm as shown in **Fig. 5** with inclination angle of 30˚ **[**45]. The substrate material was constructed from PCC and poured into the first halves of cylinders as depicted in **Fig. 1-b**. The specimens were stored at the laboratory ambient temperature of 20 ± 2 °C and 50% RH for 24 hrs and

then were cured by being covered with wet burlap up to 28 days age. After that, the GPC repair materials were applied while taking into consideration the usage of bonding agent and the surface condition. For GPC heat curing was performed for 48 hrs alternatively. The specimens were tested at the age of 3 and 28 days after applying the repair material by using a digital hydraulic compression testing machine with a capacity of 2000 kN. During loading, the interface surface is under compression and shear The applied vertical stress required to produce a failure along the bond plane can be calculated by **Eq.1**. The epoxy based resin was used as the adhesion-improving agent. For the contact surfaces, both dry and wet conditions were investigated. Only the dry surface condition was taken into consideration for the bonding agent usage.

$$\sigma_0 = P/A \qquad \textbf{Eq. 1}$$

Where:
$\boldsymbol{\sigma_0}$ is vertical stress
P = maximum load carried by the composite specimen at failure (N),
A= cross sectional area (mm^2)

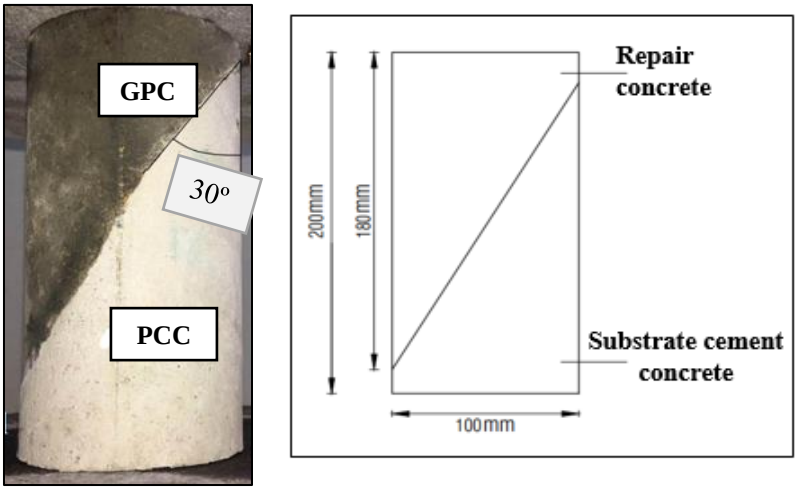

Fig. 5: Dimensions of cylindrical specimens used for slant shear test

2.3.3.2 Pull-off test

Direct tensile strength test (pull-off method) was intended to investigate the bond between the overlay material and the substrate one according to **ASTM C1583-13** [46]. The active load in this test is provided immediately perpendicular to the surface where the materials for the repair and substrate materials come into contact. The substrate material for this test was PCC prisms with (600× 150 ×75) mm. Thereafter, a layer of each repair concrete was added with thickness of 75 mm at the top of the substrate concrete at age of 28 days. The prism specimens were cured till 28 days, and then drilling core cutter had been used to make a hole of 50 mm diameter at the top surface having 112.5 mm depth through the concrete prism. The cores were drilled using core cutter measuring 45 mm, with a minimum centerline spacing of 100 mm and a minimum distance of 50 mm from the center of a disc to the free edge. After that, each core was attached to an aluminium disk using a fast setting epoxy. The epoxy was allowed to cure for 24 hrs in the lab at room temperature 20 ± 2 °C, and then pull-off device was used to manually pull off the disk at the age of 28 days until failure occurred as shown in **Fig. 6**.

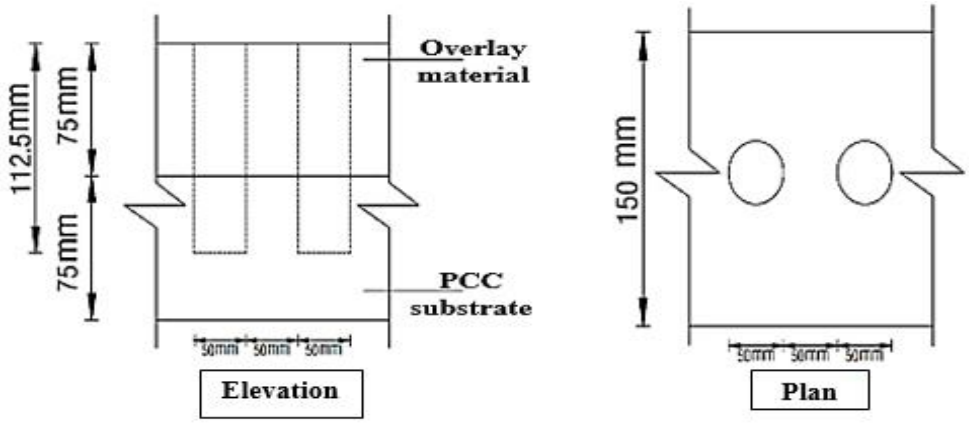

a) Scheme of pull-off specimens

b) Test device

Fig. 6: Pull-off test setup

2.3.4 Flexural performance of RC beams

The conducted RC beam specimens were subjected to flexural load by using a Universal Testing Machine of 300 kN capacities as shown in **Fig. 7**. Four-point loading test was performed for testing the RC beams. The RC beams were divided into 2 groups based on the damage level due to the loads subjected from the actuator. Fully damaged beam: one of RC beams (control beam) was loaded till failure. In this RC beam, the static load was applied to achieve the ultimate load level. And partially damaged beams: two specimens of RC beams loaded up to 45% and 75% of their ultimate load, respectively. The tests were applied gradually with rate 0.4 mm/s till the limited percentage load for every beam.

Fig. 7: Beam specimens test setup

III. Test results and discussions

3.1 Fresh test results

A slump test was conducted on each of the mixes used in the current experimental program. The FA-based GPC had a slump value of 230 mm, while the control mix, PCC, had slump value of 80 mm. Extra water and SP were added to GPC mixes including GGBFS in different proportions, as indicated in **Table 4**, in order to attain a constant slump value of 230 mm for the repair applications. Furthermore, it was found that adding more GGBFS up to 100% mix F0S100 decreased the workability and produced a stiffer mix **[**47,48]; consequently, additional extra water and SP were used.

3.2 Mechanical test results of concrete mixes

Table 5 displays the test results of mechanical properties for different concrete mixes.

Table 5: Test results of mechanical properties of different concrete mixes

Mix ID	Compressive strength (MPa)			Splitting tensile strength (MPa)		Flexural strength (MPa)		Modulus of elasticity (GPa)		Bond strength (MPa)	
	3 days	7 days	28 days	7 days	28 days	7 days	28 days	7 days	28 days	7 days	28 days
F100S0	17.4	23.5	31.2	2.3	2.8	3.2	3.9	20.3	25.3	8.7	9.9
F50S50	39	49	52.7	3.8	4.9	5	6.2	23.9	29.8	12.7	14.3
F25S75	26.1	37.9	39	3.1	3.7	3.7	4.6	21	26.2	10.7	13.5
F0S100	26.8	38.1	39	2.8	3.5	3.5	4.4	20.6	25.7	12.3	13.7
PCC	14	24	30	1.9	2.5	3.1	3.8	18.7	23.4	6.3	7.6

3.2.1 Compressive strength

Figure 8 and **Table 5** exhibit compressive strength of various concrete mixes. At 3 and 7 days, the inclusion of GGBFS causes an early strength gain in GPC. High early age strength is a desired property of concrete repair, strengthening and protective materials. F50S50, F25S75, and F0S100 strength after 3 and 7 days was found to be around (74%, 66.9%, 68.7%) and (93%, 97.2%, 97.7%) of that after 28 days, respectively.

At the age of 28 days, the compressive strength of F100S0 is lesser than the compressive strength of F50S50, F25F75 and F0S100 by percentages of 68.9%, 25% and 25%, respectively. It is discovered that when compared to a PCC mix, its compressive strength is less than that of F100S0, F50S50, F25S75, and F0S100 by percentages of 4%, 75.6%, 30%, and 30%, respectively. The maximum compressive strength is 52.7 MPa with 50% GGBFS content, while with 100% FA, the lowest is 31.2 MPa. Thus, when 50% GGBFS is used instead of FA, the percentage increase in compressive, this finding is in line with the result attained by **(Rashad, 2015)** [48].

When the 'Ca' components in GGBFS interacted, they produced more C-S-H and C-A-S-H, which coexisted with geopolymer products [49] and supported the strength development of GPC concrete. This is consistent with a different study that discovered a high pozzolanic activity and calcium content were related to a high rate of strength development.

Furthermore, this is because the presence of C-S-H gel will increase the alkalinity, accelerating the geopolymerization and dissolution of aluminosilicate [50 -52]. Because FA contains less calcium than GGBFS, the strength of the FA-based geopolymer repairing material is lower than that of the GGBFS-based geopolymer [53]. However, increased GGBFS content resulted in extra water being present and an increase in SP for workability, which decreased the compressive strength [54]. In this study, increasing the GGBFS content from 50% to 100% (F25S75 and F0S100) decreased compressive strength at various ages but still higher than PCC.

3.2.2 Splitting tensile strength

Figure 8 and **Table 5** depict the results of the splitting tensile strength test. By looking at test results as indicated in **Table 5**, it was noted the mix with 50% GGBFS content gave the best splitting tensile strength. By way of instance, replacement of FA content by 50%, 75% and 100% with GGBFS resulted in increasing of splitting tensile strength by (39.5%, 25.8%, 17.9%) and (42.8%, 24.3%, 20%), respectively, for mixes F50S50, F25S75 and F0S100 when compared with F100S0 mix at the age of 7 and 28 days.

While the splitting tensile strength for PCC mix at age of 28 days was about 2.5 MPa, and it was discovered that its strength is less than F100S0, F50S50, F25S75 and F0S100 by percentages of 12%, 96%, 48% and 40%, respectively. This finding is in line with **Hussein et al.,2021** [55].

The increase in strength with using GGBS in ambient cured GPC is attributed to the formation of the additional reaction product, calcium aluminosilicate hydrate (C-A-S–H) and (N-A-S-H) gels, resulting in pore refinement and the compactness of the microstructure **(Kumar et al., 2010)** [47] and **(Pan et al., 2018)** [56]**.**

3.2.3 Flexural strength

The flexural strength results are presented in **Table 5** and shown in **Fig. 8**. The results showed that the highest value of flexural strength at the age of 7 days reached 5 MPa for F50S50 mix, where this value is higher than F100S0, F25S75 and F0S100 by percentages of 36%, 26% and 30%, respectively. 100% FA caused a decrease in the flexural strength value by 56.3%, 15.6% and 9.4% comparing with F50S50, F25S75 and F0S100 mixes respectively.

At age of 28 days the flexural strength for F50S50 mix was about 6.2 MPa is higher than the flexural strength of F100S0, F25S75, F0S100 and PCC by percentages of 37.1%, 25,8%, 29.1% and 63.2%, respectively. It can be noted that the absence of GGBFS, the F100S0 mix had the lowest flexural strength of 3.9 MPa. So the best flexural strength was observed for F50S50 mix and it can be seen that flexural strength increased when GGBFS was used with FA with percentage 50%. These results are in agreement with previous studies [57,58]. Using GGBFS in GPC mixes enhanced the flexural strength. The increase in strength with using GGBFS in

ambient cured GPC is attributed to the formation of the additional reaction product, calcium aluminosilicate hydrate (C-A-S–H) and (N-A-S-H) gels, resulting in pore refinement and the compactness of the microstructure [47, 56].

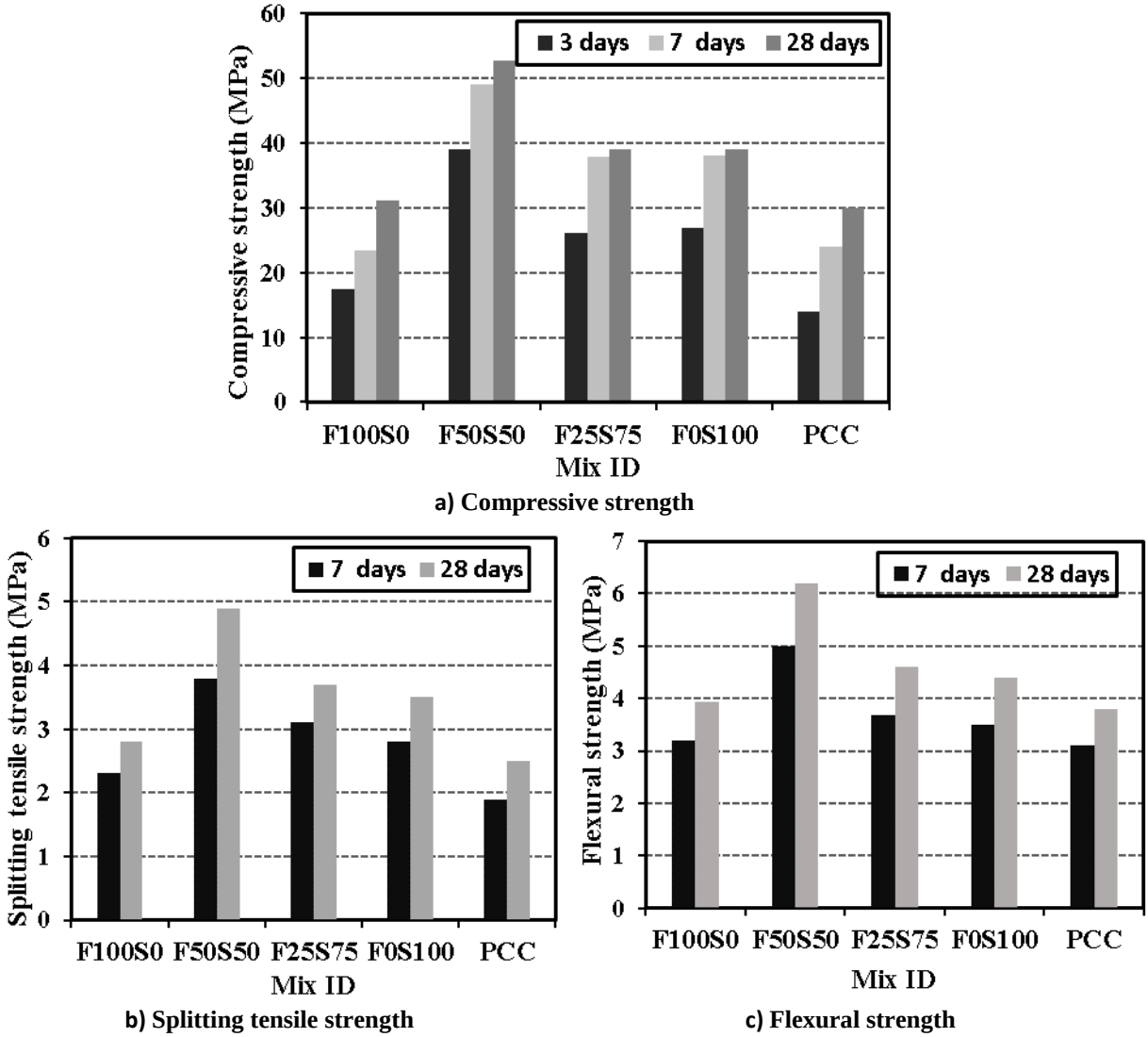

Fig. 8: Test results of compressive, splitting tensile and flexural strengths for different concrete mixes at different ages

3.2.4 Modulus of elasticity

The modulus of elasticity results are shown in **Table 5** and **Fig. 9**. The results showed that the mix with 50% GGBFS content represents the best performance for compressive strength and the amount of elongation applied to it, which results in the lowest possible strain. Thus, the highest modulus of elasticity is achieved. For instance, replacement of FA content by 50%, 75% and 100% GGBFS resulted in improving of modulus of elasticity by (14.6%, 3.3%, 1.5%) and (15.1%, 3.4%, 1.6%) respectively: for mixes F50S50, F25S75 and F0S100 when compared with F100S0 mix at the age of 7 and 28 days.

When comparing GPC mixes with PCC mix, it was found that its modulus of elasticity is greater than PCC mix by percentages of 7.5%, 21.5%, 10.7% and 8.9%, respectively: for mixes F100S0, F50S50, F25S75 and F0S100 at the age of 28 days.

Whereas **(Amin et al., 2022)** [59], proved that there is a significant improvement in the modulus of elasticity of GPC by 3.3% of PCC when adding FA and GGBFS at a ratio of 50:50. It is known that there is a direct relationship between the compressive strength and the modulus of elasticity. Accordingly, the modulus of elasticity increases with the increase in the compressive strength, and therefore the increase in the value of GGBFS reduces the modulus of elasticity in the presence of excessive addition of SP. The permissible limit and

the appropriate value of it have a great impact on the compressive strength, as mentioned by **(Boukendakdji et al., 2012)** [60].

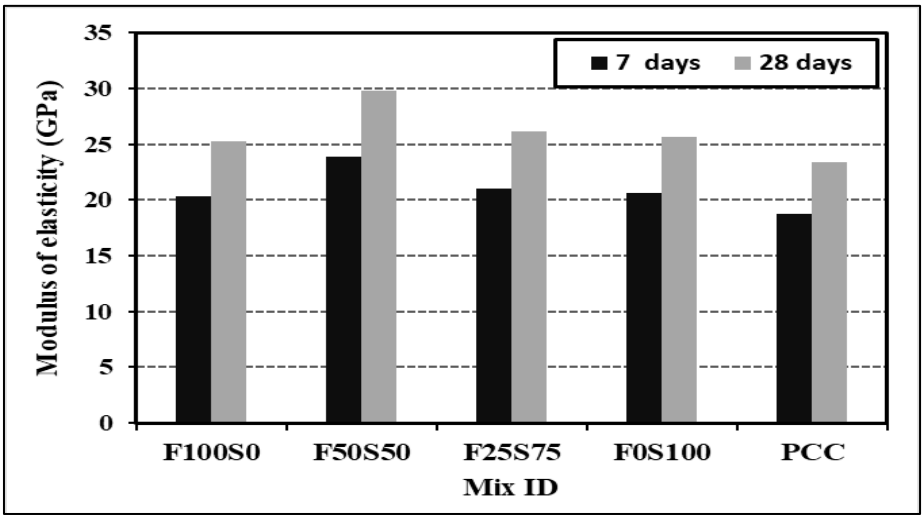

Fig. 9: Modulus of elasticity for different concrete mixes at different ages

3.2.5 Bond strength

Results from pull-out test of different concrete mixes are presented in **Table 5** and shown in **Fig. 10**. It is evident that the bond strength of mix with 50% GGBFS content is highest compared to others at 7 and 28 days. However**, Laskar and Talukdar** [28] studied bond strength of GPC as a repair material with using 50% GGBFS when comparing the results of the current study, it was found that, the bond strength increased by about 66.7% at 3 days and 43.4% at 28 days this may be due to the use of potassium silicate in the mix. The inclusion of FA with GGBFS improved particle mixing mobility that produced a homogeneous mix. As a result, the mix and rebar surface bonded more effectively. However, adding a high amount of GGBFS (>50%) led to reduced bond strength because of using SP to improve the workability with dosage higher than 1.5%, which resulted in this reduction. On the other hand, FA-based GPC has the lowest bond strength and a slower rate of strength development compared to blended GPC.

It is discovered that when compared to a PCC mix, the bond strength is less than that of F100S0, F50S50, F25S75 and F100S0 by percentages of 27.6%, 50.4%, 41.1% and 48.4% at age of 7days and by percentages of 23.2%, 46.9%, 43.7% and 44.5% at age of 28 days respectively.

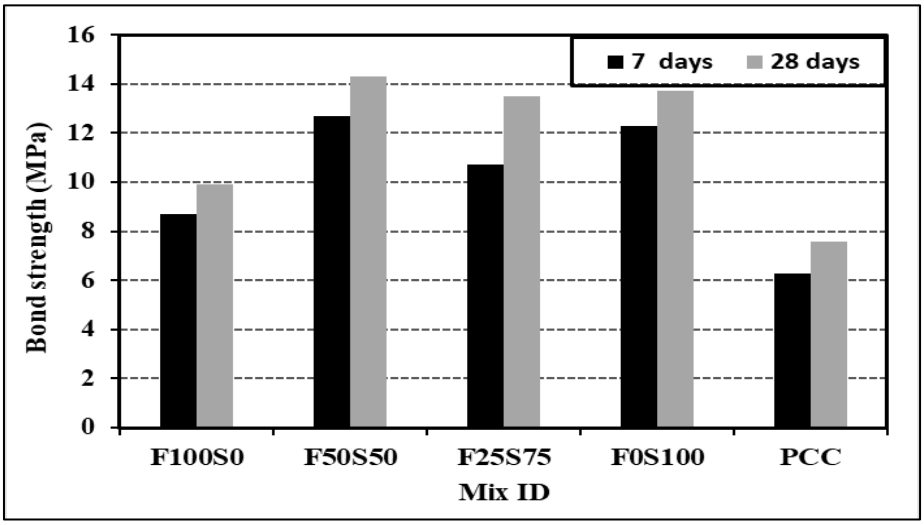

Fig. 10: Bond strength test results of different concrete mixes at different ages

Examining the specimens following their failure in the pull-out test, it was noted that there were visible wide cracks in the F25F75, F50S50 and F0S100 specimens with higher bond strengths as shown in **Fig. 11-a**, which came from the GPC mix and rebar contact and moved to the specimen's surface, demonstrating a strong bond between both. On the other hand, specimens in **Fig. 11-b** with lower bond strength failed without visible

cracks development. This demonstrated that the weak bond between the FA-based GPC mix and the rebar surface was the cause of the specimens' failure this also happened in the PCC specimens [28].

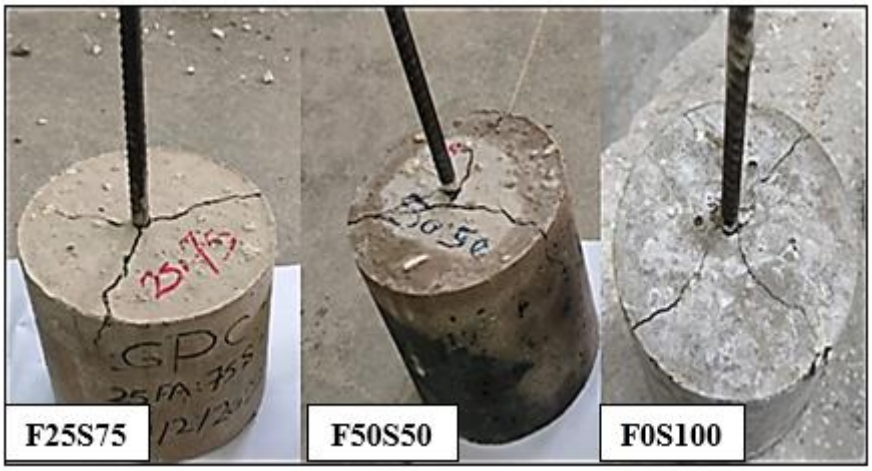

a) Specimens with visible cracks

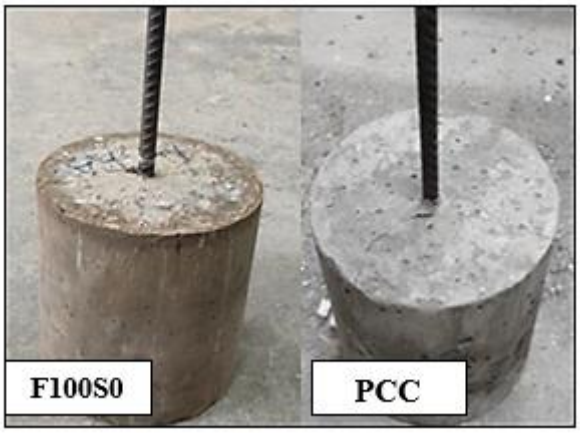

b) Specimens without visible cracks

Fig. 11: Pull-out test specimens after failure

3.3 Evaluation of Bond Strength between concrete overlay and concrete substrate

The test results of shear bond strength and tensile bond strength by using slant shear and pull-off tests, respectively are given in **Table 6** and depicted in **Figs. 12-15**.

Table 6: Test results of bond strength of GPC with PCC substrate specimens

Specimens ID	Shear bond strength (MPa)						Tensile bond strength (MPa)
	3 days			28 days			28 days
	Dry	Wet	Epoxy	Dry	Wet	Epoxy	Dry
F100S0/PCC	13.1	15.6	12.5	20.7	20.1	14.9	0.6
F50S50/PCC	20.3	18.5	16.1	29.7	26.8	17.2	1.8
F25F75/PCC	17.3	18.2	13.3	27.1	24.2	14.9	1.2
F0S100/PCC	15.9	17.6	12.5	22.7	22.1	14.5	0.8
PCC/PCC	9.7	9.3	10.8	12.3	16.7	13.2	0.01

3.3.1 Shear bond strength

The purpose of the slant shear test was to evaluate the interfacial shear bond strength between the GPC as a repair and strengthening material and PCC substrate concrete. The results from slant shear test at the age of 3 and 28 days after applying repair material are presented in **Table 6** and plotted in **Fig. 12**, noting that the age of PCC substrate concrete was 93 and 118 days and had compressive strength of 35 and 36 MPa, respectively.

Generally, using GPC as a repair and strengthening material achieves better results of shear bond strength than PCC, regardless of the surface condition.

It was noticed that, the shear bond strength of cylindrical specimens increased with using GGBFS in compared with FA-based GPC specimens. In the case of specimens F50S50/PCC with dry substrate surfaces, the shear bond strength increased by about 9.7% and 10.8 % at 3 days and 28 days, respectively than depicted in the case of wet surface case.

Regarding to combined specimens incorporating GGBFS, the improvement of shear bond strength may be due to CaO content in the primary material of GGBFS being sufficient. Because Ca2+ cations produced by the dissolution of CaO had high selectivity and reactivity, the production of C-A-S-H gel happened more quickly during the geopolymerization process, Therefore, the addition of free Ca2+ cations from the PCC substrate can also result in the formation of this gel [61]. Stated otherwise, a physical reaction involving free Ca 2+ cations from the PCC substrate's surface and the fresh blended GPC resulted in the formation of new cross-link bonds between the two materials. The bonding zone is greatly enhanced as a result of this interaction, which takes place in the interfacial transition zone, increasing the strength [61].

When compared to the dry and wet surface of GPC/PCC specimens the use of epoxy resin did not improve the shear bond strength at the interfacial zone. Among the studied specimens, F50S50/PCC achieved the highest shear bond strength (17.2 MPa) at 28 days with using epoxy resin. Besides, GPC/PCC specimens achieved higher early shear bond strength compared to the corresponding PCC/PCC specimens.

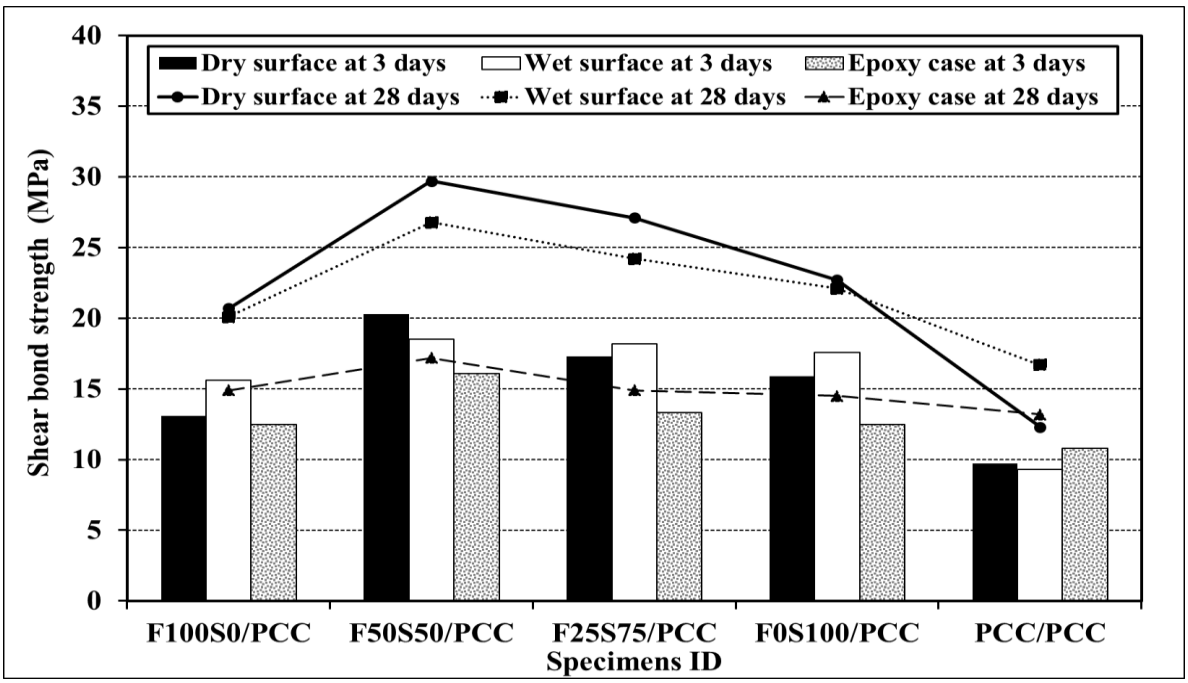

Fig. 12: Test result of shear bond strength between GPC overlay and PCC substrate with different surface condition at 3 and 28 days

The location of the failure in the specimens served as a characterization of the failure modes. The plane of failure is described as being along the interface surface when there is an interface or bond failure. Two patterns of failure, The first one happened in PCC, where the GPC was largely intact despite interface cracks that developed. This occurred in F50S50/PCC specimens in case of dry and wet surfaces, F25S75/PCC specimens in case of dry surface and F0S100/PCC specimens in case of using epoxy resin as shown in **Fig. 13**. In the monolithic mode, the slant shear bond cylinders failed. The secand type, cracks were formed in both sections of GPC and PCC substrate. This demonstrated clearly the stronger bond between the two surfaces and increased resistance to cracking of GPC. This occurred in F50S50/PCC specimens in case of using epoxy resin, F25S75/PCC specimens in case of wet surface and F100S0/PCC specimens in case of wet surface . On the other hand, for control states where one system is used to connect the other half cast with PCC as a repair material and the other half used as substrate, the failure took place in the interface layer between substrate and repair materials in all cases.

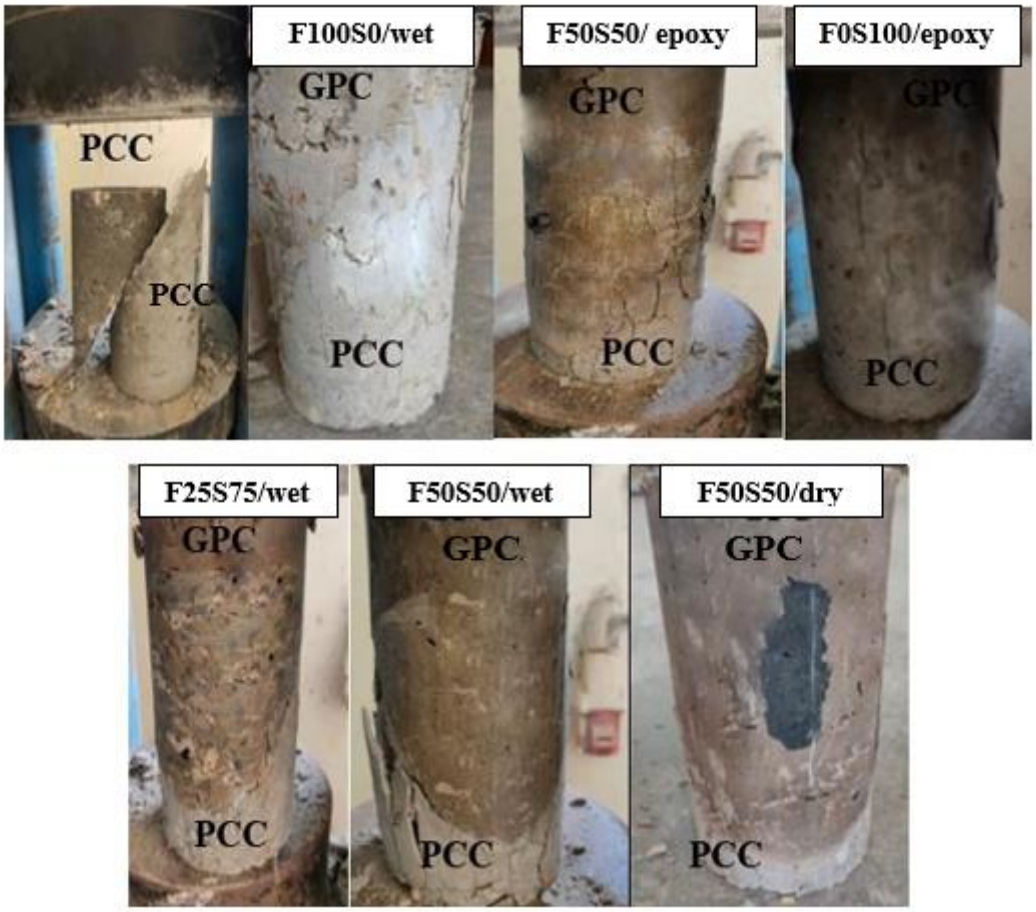

Fig. 13: Mode of failure for slant shear test specimens

3.3.2 Tensile bond strength

Table 6 and **Fig. 14** display the results of tensile bond strength for different repair materials in case dry surface which were not as accurate as the slant shear test because there is a possibility of occurs cracks or split up of the samples before testing, noting that the age of PCC substrate concrete was 93 and 118 days and had splitting tensile strength of 2.9 and 3.1 MPa, respectively. According to the findings, blended GPC with 50% GGBFS as a repair and strengthening material demonstrated a strong bond with the PCC substrate. The Pull-off test results were found to be more or less identical to that reported by different individuals [62] who investigated the tensile bond strength of the FA/GGBFS-based GPC to PCC substrate.

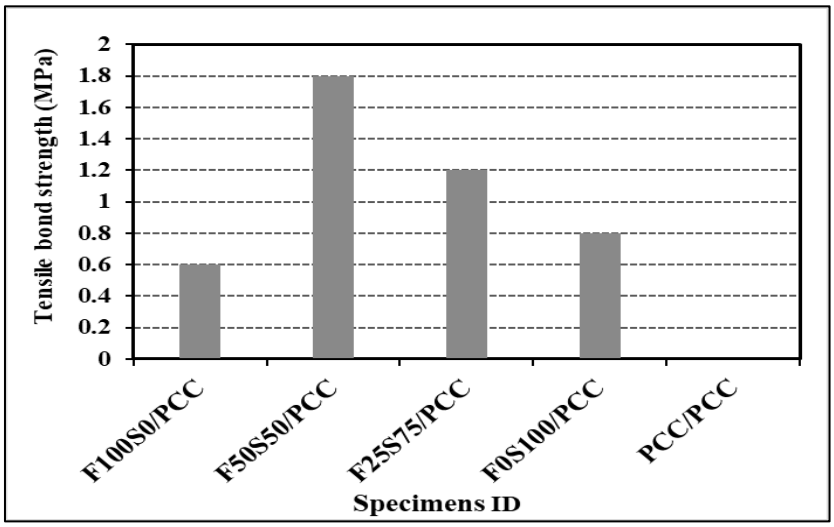

Fig. 14: Tensile bond strength between overlay and substrate concrete at 28 days

The failure modes of pull-off specimens are shown in **Fig. 15.** It was observed that failure at the contact surface between the aluminium disk and the repair materials revealed subpar epoxy, and the test was determined to be ineffective, as shown in **Fig. 15-a**, for F100S0/PCC. Additionally, F0S100/PCC specimens failed in the repair material, as depicted in **Fig. 15-b**. Howerver, F25S75/PCC specimens failed between overlay and substrate as shown in **Fig.15-c**. Besides, F50S50/PCC specimens failed at substrate concrete, as demonstrated in **Fig. 15-d.** This could be explained through the fact that the bond strength in the interfacial zone is higher than the tensile strength of the substrate. While PCC/PCC specimens broke before testing.

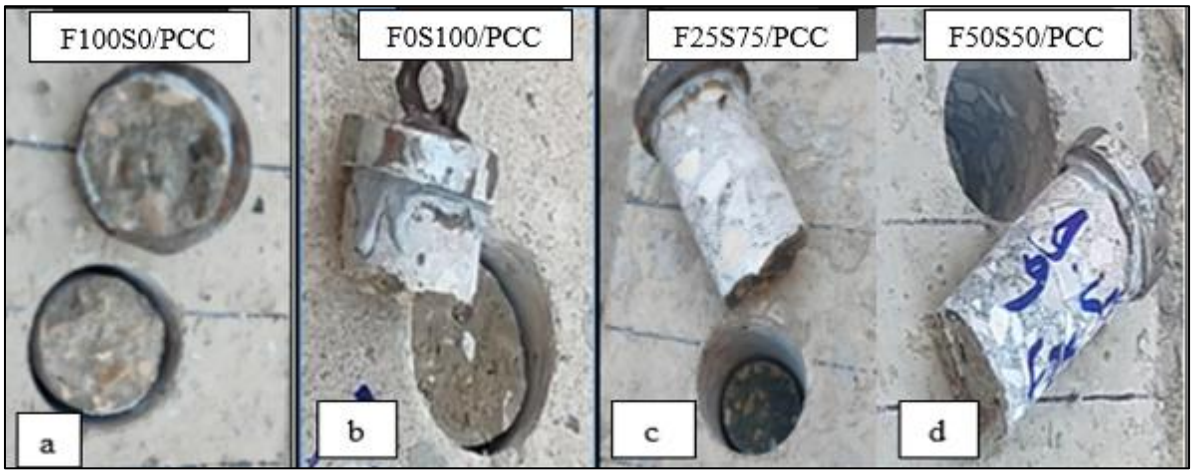

Fig. 15: Failure of the pull-off specimens a) top surface of repair material, b) repair material, c) interfacial, d) substrate concrete

3.4 Performance of reinforced concrete pre-cracked beams repaired with blended geopolymer concrete

The structural output results included the initial-cracking load (Pcr), yielding load (Py), ultimate load (Pu), mid-span deflection at the failure load (Δmax), stiffness, ductility index and toughness have been studied for different RC beams and RC beams repaired with blended GPC as given in **Table 7**. The toughness was measured as the area underneath the load-deflection curve until failure load **(Hassan et al., 2021)** [63]. The ductility index was calculated as the ratio between Δmax and the deflection at yielding load (Δy) [64]. Stiffness was defined as (P75%)/ (Δ75%) **[64**] where P75% is the load at 75% of ultimate load and Δ75% is the corresponding mid-span deflection.

Table 7: The test results for different tested reinforced concrete beam specimens

Beam ID	P_{Cr} (kN)	P_y (kN)	P_u (kN)	Δmax (mm)	Δy (mm)	Ductility index	Stiffness (kN/mm)	Toughness (kN.mm)
B100	65.3	80.8	119	3.5	1.8	1.94	34	203.4
B75	60.2	79.1	89.3*	2	1.2	1.24	45.3	53.9
B45	-	-	53.6*	1.3	-	-	41.3	18.2
B100R	47.2	58.64	76.2	6.5	2	3.24	11.7	403.6
B75R	61.7	70.65	108.2	9.5	2.4	3.9	11.4	620.2
B45R	58.1	65.5	96.3	5.02	2.2	2.3	19.2	454.6

*These RC beams were loaded up to 45% and 75% of their ultimate load. The ultimate load in this case was considered as the ultimate load of controlled beam, B100. **Pcr**: the cracking load, **Py**: the yield load, **Pu**: the ultimate load (maximum load), **Δy**: the mid-span deflection at yield load, **Δmax**: the maximum mid-span deflection at failure.

3.4.1 Load-deflection behavior of beams specimens

The load-deflection relationships for the flexural group investigated beams are shown in **Fig.16**. Each of the load deflection relationships can be divided into two stages; first stage represents a linear relationship between the applied load and the measured mid span deflection up to a certain point at which the relationship starts to behave as nonlinear. The load value at which the relationship changed from linear to nonlinear varied from beam to another. In the second stage of loading a nonlinear relationship was recorded for all tested beams up to final failure.

As presented in **Fig. 16**, repaired fully damaged RC beam (B100R) attained an ultimate load of 76.22 kN which was around 64.1% of the load attained by RC controlled beam (B100). The 1st crack occurred at 47.2

kN which was around 72.3% of the load for appearance of 1st crack in B100. Δmax for B100R was 6.48 mm as compared to 3.5 mm for RC controlled beam B100 with increasing ratio by 85.1%. Also, the repaired pre-cracked RC beams specimens B75R and B45R showed improvement in Pcr and Pu as compared to repaired RC beam specimens B100R as shown in **Fig. 16**. Pcr of repaired RC beams specimens B75R and B45R was 61.7 kN and 58.1 kN, respectively which were higher than the cracking load of repaired RC beam specimen B100R by 30.7% and 23.1%, respectively. Pu of repaired RC beams specimens B75R and B45R was 108.2 kN and 96.33 kN, respectively as compared to 76.22 kN for repaired RC beam specimen B100R with increasing ratios by 41.9% and 26.4%, respectively. From the results, it can be noticed that the efficiency of the proposed blended GPC mix for repairing and strengthening of PCC beam specimens increased with the increase in the level of pre- cracked beam specimens.

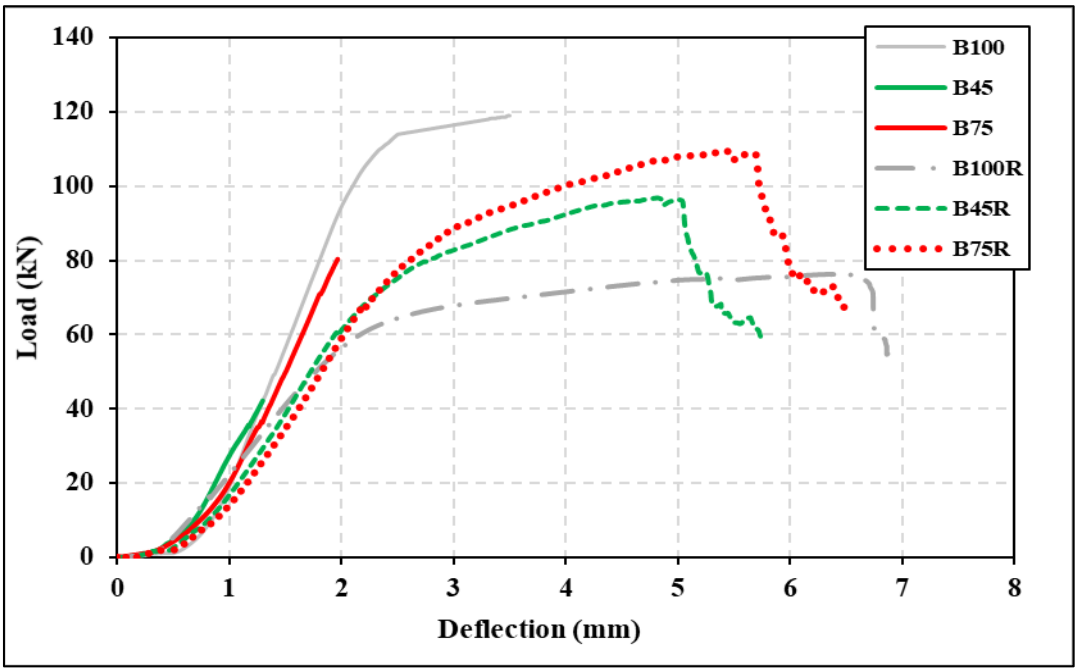

Fig. 16: Load deflection of control and repaired RC beams specimens

3.4.2 Ductility index, Stiffness and Toughness of specimens

The characteristics of substrate RC and RC repaired beams including ductility index, stiffness and toughness are presented in **Table 7** and **Fig. 17**. When comparing ductility index and toughness of RC repaired beam B100R were higher than RC controlled beam B100 by 67% and 98.4% respectively. However, the stiffness of the RC repaired beams B100R was lowered by 65.5% compared to RC controlled beam B100, these results are agreed with (**Laskar and Talukdar, 2019**) [26]**.**

RC repaired beam specimen B75R recorded higher ductility index and toughness than RC repaired beam specimens B100R and B45R by (22.2%, 72.2%) and (53.7%, 36.4%) respectively. The increase of the yield load and its corresponding deflection resulted in this reduction of the ductility ratio, as defined in this investigation.

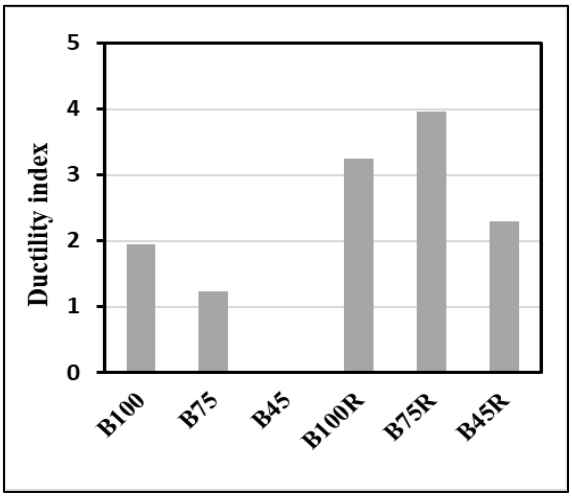

a) Ductility index

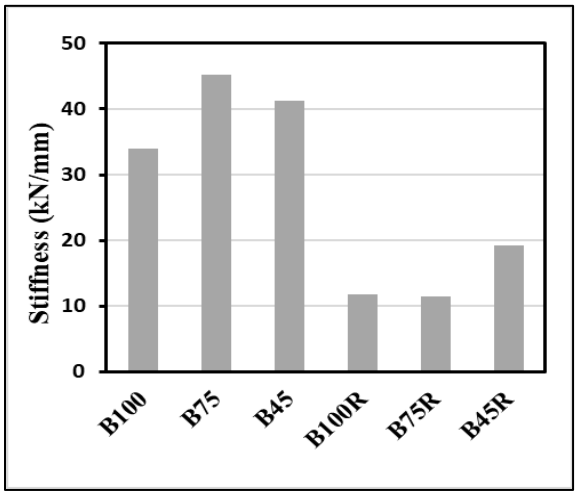

b) Stiffness

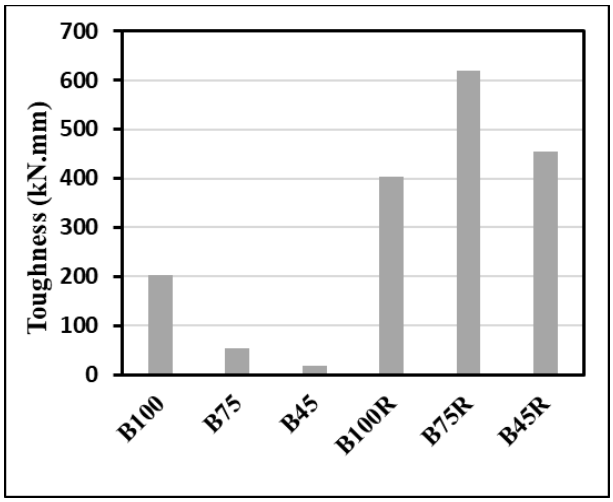

c)Toughness

Fig. 17: Structural properties of of control and repaired pre- cracked RC beams

3.4.3 Crack pattern and mode of failure of RC beam specimens

The crack patterns and mode of failure for the investigated beams are shown in **Fig. 18**. It can be observed as given in the figure and from the test follow up that the cracks started with a limited number in the tension zone of the third middle part of the beam. With increasing of the applied load, the number of cracks were increased and extended to the compression zone in addition to the neutral axis moved from tension to compression zone until the failure occurred. The cracks were vertical and in the middle of the beam and has a slightly inclined angle at the beam side, this angle varied depended on the place of crack, these results in line with (**Laskar and Talukdar,** 2019) [26].

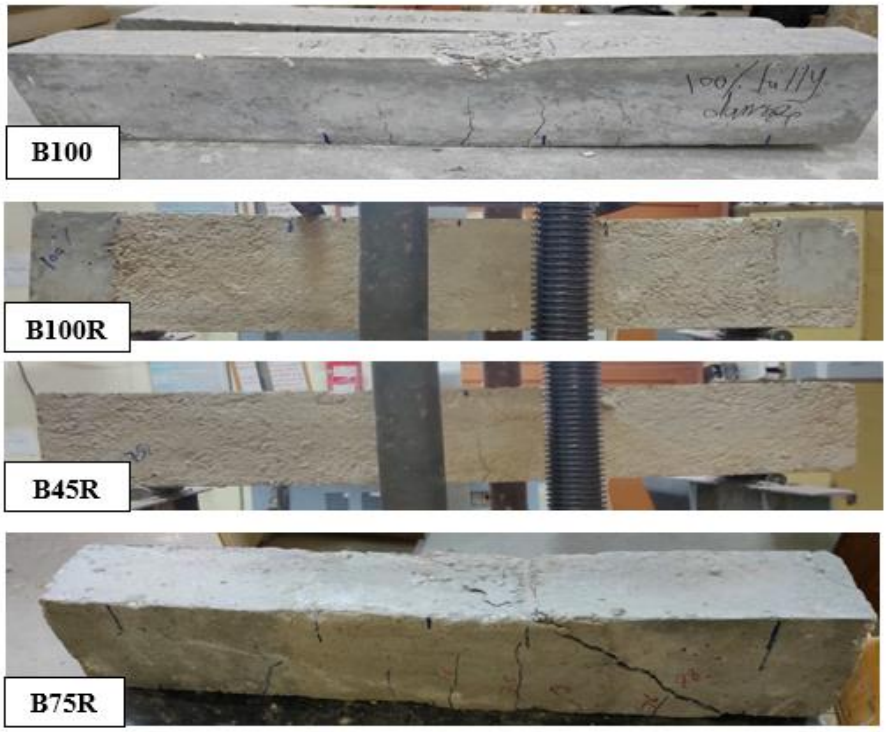

Fig. 18: Crack patterns and mode of failure for the investigated beams

IV. Conclusions

The mechanical and bonding properties of blended geopolymer concrete (GPC) as a repairing and strengthening material were investigated in this study. Based on the experimental test results, the following conclusions can be drawn:

1- The blended geopolymer repair concrete mixes showed better mechanical performance and bond strength compared to the ones with 100% FA content.

2- After looking into the mechanical properties, it was found that a GPC mix with 50% GGBFS has the best compressive strength, Flexural strength, tensile strength and modulus of elasticity and can be utilized as a repair and strengthening material in place of traditional concrete.

3- The slant shear strength of GPC increased with using GGBFS. In the case of specimens with 50% GGBFS content on dry substrate surfaces, the slant shear strengths increased by about 9.7% and 10.8 % at 3 days and 28 days, respectively than depicted in the case of wet surface case.

4- In the pull-off test, the blended GPC with 50% GGBFS demonstrated a strong tensile bond strength with the cementitious concrete under dry interface surface condition.

5- Repaired RC beam specimen B75R recorded higher ductility index and toughness than repaired RC beam specimens B100R and B45R by (22.2%, 72.2%) and (53.7%, 36.4%) respectively.

6- The performance of the repaired and strengthened beams is also significantly impacted by the level of damage. When repaired RC beams subjected to static flexural load, repaired partially damaged RC beams exhibited better behavior than repaired fully damaged RC beams.

7- Repair and strengthening of pre- cracked RC beams with GPC at the earliest stage of deterioration is recommended as it the effective way of restoring the structure to its functional use at the earliest period possible. As well as, the efficiency of the proposed blended GPC repair mix increased with the increase in the level of pre- cracked RC beam specimens.

8- Further studies are required to encourage the use of geopolymers as repairing and strengthening materials for various applications. Studying the bond strength for using replaced of FA based material by various binders (Silica Fume and Metakaolin).

Acknowledgements

The authors would like to express their appreciation to the support from the staff of the Properties of Materials laboratory- Faculty of Engineering Tanta University, Tanta, Egypt for their assistance in carrying out this study at various stages.

References

[1]. Sumesh, M., Alengaram, U.J., Jumaat, M.Z., Mo, K.H. and Alnahhal, M.F., 2017. Incorporation of nano-materials in cement composite and geopolymer-based paste and mortar–A review. Construction andBuilding Materials, 148, 62-84.

[2]. Huseien, G.F., Mirza, J., Ismail, M., Ghoshal, S.K. and Hussein, A.A., 2017. Geopolymer mortars as sustainable repair material: A comprehensive review. Renewable and Sustainable Energy Reviews, 80, 54-74.

[3]. Turner, L. K., & Collins, F. G. (2013). Carbon dioxide equivalent (CO2-e) emissions: A comparison between geopolymer and OPC cement concrete. Construction and Building Materials, 43, 125–130.

[4]. Ahmed, H. U., Mohammed, A. A., Rafiq, S., Mohammed, A. S., Mosavi, A., Sor, N. H., & Qaidi, S. M. (2021). Compressive strength of sustainable geopolymer concrete composites: a state-of-the-art review. Sustainability, 13(24), 13502.

[5]. Zannerni, G. M., Fattah, K. P., & Al-Tamimi, A. K. (2020). Ambient-cured geopolymer concrete with single alkali activator. Sustainable Materials and Technologies, 23, 23 00131.

[6]. Upadhyay, H., Mungule, M., & K. R. Iyer, K. (2022). Issues and challenges for development of geopolymer concrete. Materials Today: Proceedings, 65, 1567–1574.

[7]. Part, W. K., Ramli, M., & Cheah, C. B. (2015). An overview on the influence of various factors on the properties of geopolymer concrete derived from industrial by-products. Construction and Building Materials, 77, 370–395.

[8]. Singh, B., Ishwarya, G., Gupta, M., & Bhattacharyya, S. K. (2015). Geopolymer concrete: A review of some recent developments. Construction and Building Materials, 85, 78–90.

[9]. Mehta, A., & Siddique, R. (2016). An overview of geopolymers derived from industrial by-products. Construction and Building Materials, 127, 183–198.

[10]. Ghazy, M. F., Abd Elaty, M. A., Taman, M., & Eissa, M. E. (2022). Durability performance of geopolymer ferrocement panels prepared by different alkaline activators. In Structures (Vol. 38, pp. 168-183). Elsevier.

[11]. Mastali, M., Kinnunen, P., Dalvand, A., Firouz, R. M., & Illikainen, M. (2018). Drying shrinkage in alkali-activated binders–a critical review. Construction and Building Materials, 190, 533-550.

[12]. Ma, Y., & Ye, G. (2015). The shrinkage of alkali activated fly ash. Cement and Concrete Research, 68, 75-82.

[13]. Lee, N. K., Jang, J. G., & Lee, H. K. (2014). Shrinkage characteristics of alkali-activated fly ash/slag paste and mortar at early ages. Cement and Concrete Composites, 53, 239-248.

[14]. Zhang, Z., Yao, X., & Wang, H. (2012). Potential application of geopolymers as protection coatings for marine concrete III. Field experiment. Applied Clay Science, 67, 57-60.

[15]. Ghazy, M. F., Taman, M. H., & ELatfawy, S. S. (2022). Properties and durability of geopolymer based materials and it's utilizing as a repair and strengthening materials: a review. environment, 18, 19. International Research Journal of Engineering and Technology (IRJET)

[16]. Guo, X., & Pan, X. (2018). Mechanical properties and mechanisms of fiber reinforced fly ash–steel slag based geopolymer mortar. Construction and Building Materials, 179, 633-641.

[17]. Huseien, G. F., Mirza, J., Ismail, M., & Hussin, M. W. (2016). Influence of different curing temperatures and alkali activators on properties of GBFS geopolymer mortars containing fly ash and palm-oil fuel ash. Construction and Building Materials, 125, 1229-1240.

[18]. Ma, C. K., Awang, A. Z., & Omar, W. (2018). Structural and material performance of geopolymer concrete: A review. Construction and Building Materials, 186, 90-102.

[19]. Zhang, Z., Yao, X., & Zhu, H. (2010). Potential application of geopolymers as protection coatings for marine concrete: II. Microstructure and anticorrosion mechanism. Applied clay science, 49(1-2), 7-12.

[20]. Momayez, A., Ehsani, M. R., Ramezanianpour, A. A., & Rajaie, H. (2005). Comparison of methods for evaluating bond strength between concrete substrate and repair materials. Cement and concrete research, 35(4), 748-757.

[21]. Ghazy. M.F, Abd Elaty. M.A, Taman. M.H, Nasr. N.A. (2021). Efficiency of Interfacial Bond Technique between Geopolymer and Portland Cement Concrete Layers on the Flexural Behavior of Slabs having a Composite Section, Vol: 08 ,No: 01, pp: 2395-0072.

[22]. Hu, S., Wang, H., Zhang, G., & Ding, Q. (2008). Bonding and abrasion resistance of geopolymeric repair material made with steel slag. Cement and concrete composites, 30(3), 239-244.

[23]. Suksiripattanapong, C., Horpibulsuk, S., Chanprasert, P., Sukmak, P., & Arulrajah, A. (2015). Compressive strength development in fly ash geopolymer masonry units manufactured from water treatment sludge. Construction and Building Materials, 82, 20-30.

[24]. Ding, Y. C., Cheng, T. W., & Dai, Y. S. (2017). Application of geopolymer paste for concrete repair. Structural Concrete, 18(4), 561-570.

[25]. McAlorum, J., Perry, M., Vlachakis, C., Biondi, L., & Lavoie, B. (2021). Robotic spray coating of self-sensing metakaolin geopolymer for concrete monitoring. Automation in Construction, 121, 103415.

[26]. Laskar, S. M., & Talukdar, S. (2019). A study on the performance of damaged RC members repaired using ultra-fine slag based geopolymer mortar. Construction and Building Materials, 217, 216-225.

[27]. Zhang, H., & Hadi, M. N. (2019). Geogrid-confined pervious geopolymer concrete piles with FRP-PVC-confined concrete core: Concept and behaviour. Construction and Building Materials, 211, 12-25.

[28]. Laskar, S. M., & Talukdar, S. (2017). Preparation and tests for workability, compressive and bond strength of ultra-fine slag based geopolymer as concrete repairing agent. Construction and building materials, 154, 176-190.

[29]. Carabba, L., Santandrea, M., Carloni, C., Manzi, S., & Bignozzi, M. C. (2017). Steel fiber reinforced geopolymer matrix (S-FRGM) composites applied to reinforced concrete structures for strengthening applications: A preliminary study. Composites Part B: Engineering, 128, 83-90.

[30]. Wasim, M., Ngo, T. D., & Law, D. (2021). A state-of-the-art review on the durability of geopolymer concrete for sustainable structures and infrastructure. Construction and Building Materials, 291, 123381.

[31]. ASTM C618-12, "Standard Specification for Coal Fly Ash and Raw or Calcined Natural Pozzolan for Use in Concrete," American Society of Testing Materials.

[32]. ASTM C989-94, "Standard specification for ground granulated blast-furnace slag for use in concrete and mortars," American Society of Testing Materials.

[33]. EN 196-1:2016 – Cement – Part 1: Methods of testing cement-part1: Determination of strength. European Committee for standardization, Brussels, Belgium

[34]. ES 4756 (2022) Cement part 1 composition, specific and conformity criteria for common cements. Egyptian Organization for Standards & Quality. Egypt

[35]. ECP-203: 2020. Egyptian Code of Practice for Design and Construction of Reinforced Concrete Structures. Appendix 3. Housing and Building Research Center, Ministry of Building and Construction, Egypt
[36]. ASTM C33/C33M-18, (1994), Standard Specification for concrete aggregates, vol. 4.02. American Society of Testing Materials.
[37]. Ghazy, M., Abd Elaty, M., Taman, M., & Eissa, M. (2022). Fresh and mechanical properties of fly ash-based geopolymer mortars activated by different alkaline solutions. International Journal of Advances in Structural and Geotechnical Engineering, 5(02), 24-39.
[38]. ES 262-1 (2015) Steel for the reinforcement of concrete Part 1:- Plain bars. Egyptian Organization for Standards & Quality. Egypt.
[39]. McAlorum, J., Perry, M., Vlachakis, C., Biondi, L., & Lavoie, B. (2021). Robotic spray coating of self-sensing metakaolin geopolymer for concrete monitoring. Automation in Construction, 121, 103415.
[40]. ASTM C143 / C143M - 15a, (2009), "Standard test method for slump of hydraulic cement concrete", American Society of Testing Materials.
[41]. BS. EN-12390-3 2019. Testing hardened concrete. Compressive strength of test specimens. British Standard.
[42]. ASTM C39 / C39M - 18 "Standard test method for compressive strength of cylindrical concrete specimens", American Society of Testing Materials.
[43]. ASTM C78 / C78M - 18 "Standard test method for flexural strength of concrete" (Using simple beam with third-point loading). American Society of Testing Materials.
[44]. ASTM C882/C882M. Standard test method for bond strength of epoxy-resin systems used with concrete by slant shear. American Society of Testing Materials.
[45]. Zanotti, C., Borges, P. H., Bhutta, A., & Banthia, N. (2017). Bond strength between concrete substrate and metakaolin geopolymer repair mortar: Effect of curing regime and PVA fiber reinforcement. Cement and Concrete Composites, 80, 307-316.
[46]. ASTM-C1583/C1583M-13, Standard test method for tensile strength of concrete surfaces and the bond strength or tensile strength of concrete repair and overlay materials by direct tension (pull-off method), American Society for Testing Materials.
[47]. Kumar, S., Kumar, R., & Mehrotra, S. P. (2010). Influence of granulated blast furnace slag on the reaction, structure and properties of fly ash based geopolymer. Journal of materials science, 45, 607-615.
[48]. Rashad, A. M. (2015). A brief on high-volume Class F fly ash as cement replacement–A guide for Civil Engineer. International Journal of Sustainable Built Environment, 4(2), 278-306.
[49]. Sherwani, A. F. H., Younis, K. H., & Arndt, R. W. (2022). Fresh, Mechanical, and Durability Behavior of Fly Ash-Based Self Compacted Geopolymer Concrete: Effect of Slag Content and Various Curing Conditions. Polymers, 14(15), 3209.
[50]. Somna, K., Jaturapitakkul, C., Kajitvichyanukul, P., & Chindaprasirt, P. (2011). NaOH-activated ground fly ash geopolymer cured at ambient temperature. Fuel, 90(6), 2118-2124.
[51]. Sumajouw, D. M. J., Hardjito, D., Wallah, S. E., & Rangan, B. V. (2007). Fly ash-based geopolymer concrete: Study of slender reinforced columns. Journal of Materials Science, 42(9), 3124–3130.
[52]. Al-Majidi, M. H., Lampropoulos, A., & Cundy, A. B. (2017). Steel fibre reinforced geopolymer concrete (SFRGC) with improved microstructure and enhanced fibre-matrix interfacial properties. Construction and Building Materials, 139, 286-307.
[53]. Hammad, N., El-Nemr, A., & Hasan, H. E. D. (2021). The performance of fiber GGBS based alkali-activated concrete. Journal of Building Engineering, 42, 102-464.
[54]. Palomo, Á., Kavalerova, E., Fernández-Jiménez, A., Krivenko, P., García-Lodeiro, I., & Maltseva, O. (2015). A review on alkaline activation: new analytical perspectives.
[55]. Hussein, S. S., & Fawzi, N. M. (2021). Influence of using various percentages of slag on mechanical properties of fly ash-based geopolymer concrete. Journal of Engineering, 27(10), 50-67.
[56]. Pan, Z., Tao, Z., Cao, Y. F., Wuhrer, R., & Murphy, T. (2018). Compressive strength and microstructure of alkali-activated fly ash/slag binders at high temperature. Cement and Concrete Composites, 86, 9-18.
[57]. Ghazy M., Abd Elaty M. and El- Khouli H., (2017), "Flexural Behavior of Fibrous Reinforced Geopolymer Concrete Beams", International conference on advances in structural and geotechnical engineering (ICASGE"17), Hurghada, Egypt.
[58]. Nath, P., & Sarker, P. K. (2017). Flexural strength and elastic modulus of ambient-cured blended low-calcium fly ash geopolymer concrete. Construction and Building Materials, 130, 22-31.
[59]. Amin, M., Elsakhawy, Y., Abu el-hassan, K., & Abdelsalam, B. A. (2022). Behavior evaluation of sustainable high strength geopolymer concrete based on fly ash, metakaolin, and slag. Case Studies in Construction Materials, 16, e00976.
[60]. Boukendakdji, O., Kadri, E. H., & Kenai, S. (2012). Effects of granulated blast furnace slag and superplasticizer type on the fresh properties and compressive strength of self-compacting concrete. Cement and concrete composites, 34(4), 583-590.
[61]. Ahmad Zailani, W. W., Bouaissi, A., Abdullah, M. M. A. B., Abd Razak, R., Yoriya, S., Mohd Salleh, M. A. A., Rozainy MAZ, M. R., & Fansuri, H. (2020). Bonding strength characteristics of FAbased geopolymer paste as a repair material when applied on opc substrate. Applied Sciences, 10(9), 3321.
[62]. Lee, N. K., Kim, E. M., & Lee, H. K. (2016). Mechanical properties and setting characteristics of geopolymer mortar using styrene-butadiene (SB) latex. Construction and Building Materials, 113, 264-272.
[63]. Hassan, A., Baraghith, A. T., Atta, A. M., & El-Shafiey, T. F. (2021). Retrofitting of shear-damaged RC T-beams using U-shaped SHCC jacket. Engineering Structures, 245, 112892.
[64]. Ghazy, M. F., Abd Elaty, M. A., & Zalhaf, N. M. (2023). Performance of Normal Strength Concrete Slab Strengthened with High-Performance Concrete After Exposure to Elevated Temperature. Fire Technology, 1-39.